Available online at BCREC website: https://bcrec.id

Bulletin of Chemical Reaction Engineering & Catalysis, 18 (3) 2023, 473-484

Research Article

Effect of Particle Size of Rice-Husk Derived Silica on the Pyrolysis of Pomelo Peels

Karakate Bo-ongcharoenlab[1], Iyarin Tongdang[1], Worapon Kiatkittipong[1], Adisak Jaturapiree[2,*], Kanjarat Sukrat[2], Thanunya Saowapark[2], Ekrachan Chaichana[2]

[1]Department of Chemical Engineering, Faculty of Engineering and Industrial Technology, Silpakorn University, Nakhon Pathom 73000, Thailand.
[2]Reasearch Center of Natural Materials and Products, Chemistry Program, Faculty of Science and Technology, Nakhon Pathom Rajabhat University, Nakhon Pathom, 73000, Thailand.

Received: 3rd August 2023; Revised: 13th September 2023; Accepted: 13th September 2023
Available online: 26th September 2023; Published regularly: October 2023

Abstract

Silica with two different sizes i.e. microsilica (MS) and nanosilica (NS) was used as a catalytic support for vanadium (5-15 wt%) in the pyrolysis of pomelo peels. Besides use of pomelo peels (agricultural residues) as a feedstock for the pyrolysis, to contribute to environmental sustainability, rice husk was used as a silica source for obtaining the silica support. From the result, it was found that non-catalytic pyrolysis of pomelo peels gave a bio-oil yield of 33.3 wt%. The catalytic pyrolysis with vanadium-modified silica decreased the bio-oil yields ranging between 27.2-33.1 wt%. This was due to the occurrence of the second reactions generated from the active sites on the catalysts, which leads to the conversion of bio-oil into gas products. For NS catalyst, increasing the amount of vanadium loading directly decreased the bio-oil yields and increased the gas yield. The variation of product phase distribution was not clearly observed for MS catalyst even with various vanadium loadings. In addition, NS catalyst exhibited higher efficiency in reducing the acid content in the bio-oil, and increasing the phenol content. The distinguished properties of the nanoparticles may be the main reason for these phenomena.

Keywords: Nanotechnology; Pyrolysis; Pomelo peels; rice husk; vanadium-modified silica

How to Cite: K. Bo-ongcharoenlab, I. Tongdang, W. Kiatkittipong, A. Jaturapiree, K. Sukrat, T. Saowapark, E. Chaichana (2023). Effect of Particle Size of Rice-Husk Derived Silica on the Pyrolysis of Pomelo Peels. *Bulletin of Chemical Reaction Engineering & Catalysis*, 18(3), 473-484 (doi: 10.9767/bcrec.19801)

Permalink/DOI: https://doi.org/10.9767/bcrec.19801

1. Introduction

Agricultural residues are one of the major environmental problems in developing countries. Dumping or burning them in public places result in soil contamination, air pollution and water pollution when leached into a water source [1–3]. For pomelos, the large citrus fruit usually cultivated and consumed throughout Southeast Asia, their unusable thick peels are weighted about 40% of the fruit (1-2 kg). About 8 M metric tons of pomelo are annual produced worldwide [4], therefore an enormous amount of pomelo peels will be left and could cause environmental impacts if inappropriate disposal occur. Due to the main content of pomelo peels including cellulose, they can be applied for cellulose production application [5–7]. In addition, the relatively high content of cellulose and low amount of lignin [8] makes pomelo peels an attractive candidate for bio-oil production through a pyrolysis process. This is because cellulose can enhance the ignition characteristics of pyrolytic processes [9]. The opposite is true for lignin with more aromatic compounds. Therefore, the

* Corresponding Author.
Email: adisak@webmail.npru.ac.th (A. Jaturapiree);
Telp: +66-66-034261060, Fax: +62-034261065

pyrolysis of pomelo peels has previously been investigated along with other agricultural residues [10].

Bio-oil obtained from the pyrolysis of biomass is considered a renewable fuel to replace consumable fossil fuels. However, the bio-oil are highly acidic and corrosive, resulted from oxygenated organic compounds including carboxylic acid and carbonyl compounds [11–13]. To decrease those compounds, catalysts with acid properties which provide some specific reactions such as deoxygenation and dehydration should be introduced during the pyrolysis [14]. Various types of catalysts, including ZSM-5 [15], FCC [16], HZSM-5 [17], Y-zeolite [18], and $Ca(OH)_2$ [19], are used in the catalytic pyrolysis. Cheap materials and wastes are also used in order to reduce cost of production and environmental issues, for example; corn cob-derived activated carbon [20], *Choerospondias axillaris* seed biochar [21], and red mud [22].

Silica (SiO_2) is abundant and cheap, and can be produced from agricultural residues such as rice husk. It is frequently applied in catalytic reaction due to high strength, high abrasion and chemical resistance, and durability [23]. Even inertness, it can be modified with other components to achieve specific catalytic properties. Vanadium is one of the metals previously used as a modifier for the catalytic pyrolysis of biomass [24–26], which exhibited improving for activity and selectivity of the pyrolysis products. In addition, the advantage of nanotechnology nowadays leads using of nanoscale materials instead of conventional microscale materials. As a result, nano-silca is chosen for many applications including as a catalytic support for the particular reactions. For example, in the polymerization with metallocene, nano-silica highly interacted with the catalytic species on it, and thus can initiate the polymerization reaction with moderate catalytic activities [27]. In that study, it was also found that the effect of particle size existed even for the slightly different particle sizes. The other catalytic reactions using the nano-silica were such as *in situ* polymerization with Ziegler-Natta catalyst [28], syngas production [29], desulfurization [30], and so on [31–33]. However, there are only few studies concerned on using nano-silica for the catalytic pyrolysis of biomass. For instance, Guo *et al*. [34] have employed nano-silica modified with Ni for acetic acid steam reforming in order to utilize the biomass-pyrolyzed bio-oil in the hydrogen production. The catalyst showed the high activity with carbon conversion of 95.3% and H_2 yield of 2.38 mol.

Therefore, in this study, the catalytic pyrolysis of pomelo was conducted with nano-silica as a support modified with vanadium in various concentrations. In order to investigate the effect of support size, micro-silica were also used to compared with nano-silica. Rice husk was brought for silica extraction to obtain silica here, complied with utilization of agricultural residues as same as the production of bio-oil from pomelo peels. Micro-silica was first prepared from the rice husk, and then nano-silica was consequently synthesized from the micro-silica via a precipitation method. The prepared catalysts were characterized with various techniques such as X-Ray diffraction analysis (XRD), X-ray fluorescence (XRF), and scanning electron microscopy (SEM). The obtained bio-oils were determined for their yields, and their qualities including physical properties and chemical compositions. The effects of the catalysts on the pyrolysis process and the bio-oil quality were further discussed.

2. Materials and Methods

2.1 Materials

Rice husk and pomelo peels were donated from local areas in Nakhon Pathom province, Thailand. Hydrochloric acid (HCl, 37%) and sodium hydroxide (NaOH) were purchased from RCI Limited, New Zealand. Ammonium metavanadate (NH_4VO_3) were obtained from QRëC, New Zealand.

2.2 Preparation of catalyst

2.2.1 Micro-silica

Micro-silica was prepared from the rice husk by soaking it into the water for 1 day, filtered and then soaked in 1 M hydrochloric at 80 °C for 1 h. The soaked rice husk was washed, neutralized and dried overnight in the oven. The prepared rice husk was then calcined under atmosphere at 700 °C for 5 h to obtain the powder-like ash which was practically designated as MS.

2.2.2 Nano-silica

The prepared MS was brought to mixed with 1.5 M NaOH at the ratio of 1:6, shaken, and heated at 100 °C for 1 h. The mixture was then centrifuged and filtrated. The filtrate was then reprecipitated with 1 M HCl, adjusted the pH around 7.0-7.5, heated at 50 °C for 5 h. The solid precipitate was then washed with water, and a silica-water slurry was detected for conductivity generated by the leaving ion such as

Cl^- and Na^+. The washing step was repeated until no conductivity detected in the slurry. The solid from that process was dried at 80 °C for 10 h, ground and weighted. The obtained material was designated as NS.

2.2.3 Silica modified with vanadium

Both types of silica were modified with vanadium by incipient wetness impregnation with ammonium vanadate (NH_4VO_3). The certain amount of NH_4VO_3 solution was drop in the silica, dried at 120 °C for 1 h and then calcinated at 565 °C for 7 h. The obtained catalysts were designated as MS/VX for vanadium-modified MS, and NS_VX for vanadium-modified NS, with X identifying its vanadium content.

2.3 Pyrolysis

The catalytic pyrolysis of pomelo peels was performed in a 0.5 L bath reactor, operating at 500 °C for 2 h. with heating rate of 12.33 °C/min. 100 g of pomelo peels was packed in the reactor with 10 g of the catalyst above separated by quartz wool. N_2 was used as a carrier gas with a gas flow rate 170 mL/min, and was purge for approximately 5 minutes to remove the internal oxygen prior the pyrolysis. The outlet of the reactor was connected to two condenser set-ups and both two condenser set-ups were connected to coolant. The bio-oil product was condensed in round bottom flasks in the ice bath. After the completion of the operation, the remained solid in the reactor was allowed to cool and then weighted to determine the product yield.

2.4 Characterizations

2.4.1 Catalyst

Morphology: The morphology was investigated using Tescan Mira3 Scanning electron microscope. No coating was used to avoid interference from the coating element. Transmission electron microscope (TEM) was also used to determine the particle size of the nano-silca particle, using JEOL-TEM 200CX transmission electron spectroscopy. The sample was dispersed in ethanol to obtain the uniform dispersion prior to the measurement.

BET surface area: The surface area of silica was determined by nitrogen physisorption technique using Micromeritics ASAP 2020 surface area and porosity analyzer. The catalyst sample was thermally heated at 150 °C for 1 h before nitrogen adsorption at temperature of –196 °C.

Chemical composition: The chemical composition of silica was measured using X-ray fluorescence (XRF) with PANalytical MiniPal 4 EDXRF spectrometer, equipped with a 30 kV rhodium anode tube with a helium purge facility. A high-resolution silicon drift detector was used to count x-rays intensity. Matrix corrections were made by using either a ratio to the Compton peak or theoretical alpha coefficients, using minipal 4 software.

Acidity: The acidity was measured using a titration method [35]. The catalyst (0.1 g) was added into 50 mL of NaOH (0.05 M), shaken for 24 h and then separated with centrifugation. 10 mL of solution was added with one drop of phenolphthalein and titrated with HCl solution (0.05 M), until became transparent. Finally, the acidity was calculated as follows;

$$Acidity\,(mol.NaOH/g.cat) = \frac{(mol\,of\,NaOH)_{initial} - \left[(mol\,of\,HCl)_{added} \times 5\right]}{g\,of\,catalyst} \quad (1)$$

2.4.2 Bio-oil

Product yield: Products from pyrolysis included of 3 phases: liquid (bio-oil), solid (char) and gas. The percentage of product yield was calculated as follows;

$$Product\ yield\,(wt\%) = \frac{g\,of\,each\,phase}{g\,of\,total\,product} \times 100\% \quad (2)$$

Chemical composition: Types of compounds in the bio-oil were analyzed using GCMS technique with Thermo Scientific (TG-5MS) equipped with a capillary polar wax column, polyethylene glycol (PEG)-coated (length of 30m, internal diameter of 0.25 mm and film thickness of 0.25 mm). The conditions used were as follows: injection volume of 0.2 mL, oven at 40 °C (1 min) and continued with heating rate of 10 °C min^{-1} to 300 °C, split mode with a ratio of 100:1 and injection temperature of 290 °C. For the conversion to phenol reported, it was calculated as follows;

$$Conversion\,to\,phenol\,(\%) = \frac{wt\%\,of\,phenol}{wt\%\,of\,total\,phenolic\,compound} \times 100\% \quad (3)$$

3. Results and Discussion

3.1 Characterization of Catalyst

Rice husk was calcined to obtained white powder of silica named as MS. After that, the MS was precipitated with an acid (HCl). The smaller particles of silica which should has size in nanoscale was then produced (nanosilica, NS). Both types of silica were analysed with a scanning electron microscope

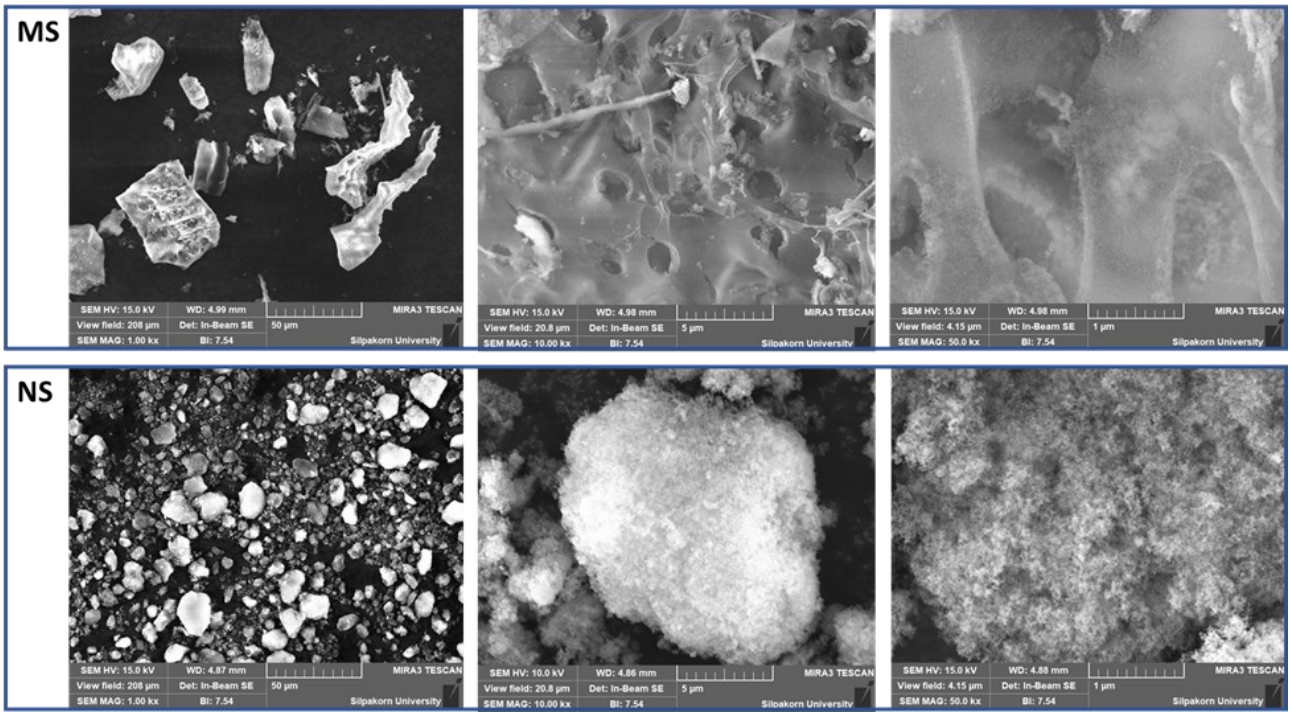

Figure 1. SEM micrographs of MS and NS at various magnification levels.

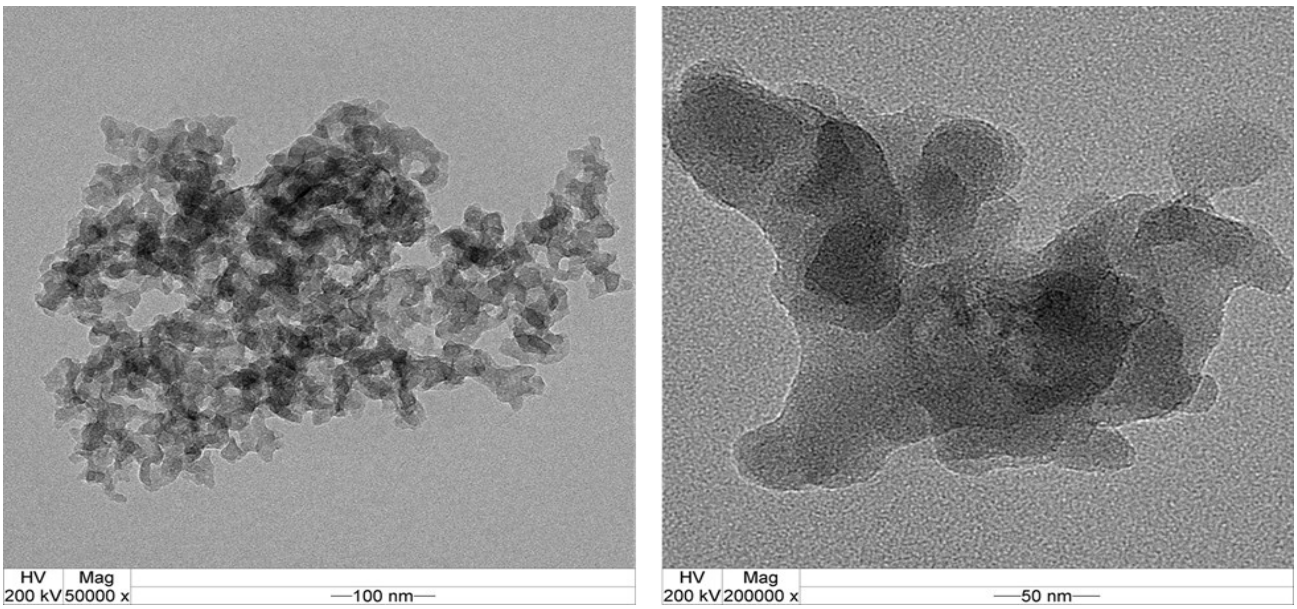

Figure 2. TEM image of NS at various magnification levels.

Table 1. Acidity of catalysts and product yields of the obtain bio-oils from the pyrolysis of pomelo peels with various catalysts.

Run	Catalyst	Acidity of catalyst (mmol.NaOH/g cat)	Product yield (wt%)		
			Liquid	Solid	Gas
1	-	-	33.3	31.3	35.4
2	MS_V5	18.3	32.5	31.5	36.0
3	MS_V10	20.3	30.3	30.8	38.9
4	MS_V15	20.5	32.4	32.4	35.2
5	NS_V5	18.7	33.1	30.9	36.0
6	NS_V10	19.1	28.0	32.3	39.7
7	NS_V15	20.2	27.2	31.5	41.3

(SEM), and their SEM micrographs are shown in Figure 1. It was found that MS exhibited irregular particles, which were larger than those of NS. For NS when observing at the low magnification level, it showed spherical-like particles with various sizes up to ~10 mm. At the higher magnification level, it was seen that the individual (secondary) particles composed of the small primary particles with sizes ranging within the nanoscale (<100 nm). These agglomerated nanoparticles may perform distinguishing characteristic of nanomaterial during the pyrolysis reaction. From the BET measurement in Table 1, NS exhibited the larger surface area and the smaller average pore size than MS as usual due to the smaller particles. The pore volume of NS was nearly the same as that of MS in a trade-off between more internal pore volume reached from the higher number of nanoparticles, and less volume from the broken of microparticles.

To support that NS has the particle size in nanometer scale as expected, a TEM technique was performed to disclose it. The TEM image in Figure 2 displayed a bunch of spherical-like particles, thus the agglomeration of the primary particles still existed. However, it can be observed that those NS particles had size ranging between 50-100 nm in according to the definition of nanoparticles.

Crystal structures of the silica were investigated using an XRD technique, and the XRD patterns of MS and NS are shown in Figure 3. It can be seen that both types of silica still exhibited nearly similar XRD patterns with a broad peak at 2θ = 22° attributed to typical amorphous silica. Small peaks at 2θ = 30.91° and 45.08° were only observed for NS. In general, there has been concern about using silica particles extracted from natural resources, which usually contains metal impurities, and thus not favorable for advanced scientific and industrial applications [36]. In addition, the process to generate nano-silica through the precipitation method with NaOH and HCl could leave some impurities remained onto the silica surface, and cause the mentioned problem.

From the experimental test, it was found that without rewashing the nanoparticle by water, the XRD pattern of the prepared silica (a small picture in Figure 3) showed the intense sharp peaks at 2θ = 30.91° and 45.08° indicating to NaCl leaving in it [37]. After the washing and being proved that there was no ion leaching to the rinsed water by a conductometer, it was observed that NS still had some typical peaks of NaCl with low intensity. This suggests that it may located inside the crystal lattice and cannot be easily removed. From the XRF measurement, it was found that MS had a SiO_2 content of 98.00% while NS has a lower one of 97.42 with Cl content of 1.87%. The impurity changed the crystal structure of the material as seen, and could slightly influence their catalytic performance. Therefore, the preparation method of silica should be carefully conducted to avoid inefficient catalyst for further using in the catalytic reaction.

The crystal structure change after vanadium impregnation was also determined as the result shown in Figure 4 [38]. It was observed that for MS with every vanadium loading, the

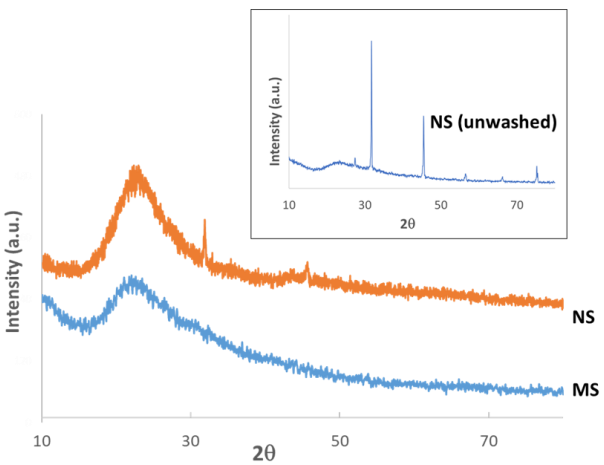

Figure 3. XRD patterns of MS, NS and NS (unwashed).

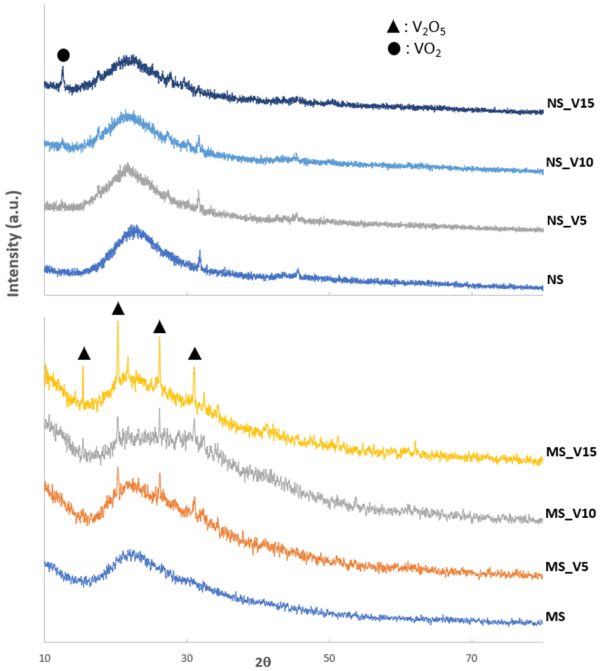

Figure 4. XRD patterns of MS and NS with various vanadium contents.

vanadium could not be well dispersed and formed as vanadium oxide (V_2O_5) in the silica. For NS, only the highest vanadium loading (at 15%) exhibited the existence of vanadium (VO_2) in the structure. This reveals that the larger surface of NS makes the vanadium better dispersed than that of the lower surface of MS. Change in oxidation states of vanadium (V^{3+} and V^{4+}) upon the silica with different particle sizes was also exposed here.

3.2 Pyrolysis of Pomelo Peels

The pyrolysis of pomelo peels was conducted along with no catalyst and two types of catalysts *i.e.* MS and NS with various vanadium concentrations. The product distributions from all pyrolysis systems are shown in Table 1. It can be seen that for all catalytic pyrolysis systems (runs 2-7) they gave the lower liquid yield than that of the conventional pyrolysis (run 1), while the solid yields were all nearly similar in all systems. The decrease of liquid yield was due to the catalytic reactions such as decarboxylation and decarbonylation, leading the intermediate vapor to be smaller molecules and gas products. In addition, cracking organic compounds into light gases could also be derived from the strong acid sites of the catalyst. The reduction of liquid yields with the catalysts is commonly found in many catalysts, for example MgO [39], activated carbon [40], and Ni-carbon [41]. Besides the catalytic reactions taking place due to the presence of the catalyst, Fang *et al*. [39] suggested that adding the catalyst (MgO) could also decreased the activation energy and increased the cracking rate.

It was observed that the NS was more efficient to generate the catalytic reaction than the MS. Nanoparticles of alumina (Al_2O_3) has also been reported to have the remarkable ability as a catalytic support for metals (Ni, Fe, Cu, Zn and Mo) to perform catalytic reactions (deoxygenation) during the pyrolysis of pine needle biomass [42]. In addition, the effect of vanadium concentration was apparently exerted for the NS only, as the bio-oil yield decreased with increasing the vanadium content. Change in oxidation state of vanadium between MS and NS could be one of the factors affecting their catalytic performance. In addition, from many literatures, the benefit of nanoparticle size on the catalytic activity are attributed to high surface-to-volume ratio, lower activation energy [43], and unique adsorption ability [44]. High surface of the nano supports could make the space for each active site of the catalysts to stay far away, leaving them easy to be attacked by the vapor molecules. On the other hand, for MS with over vanadium loading impels the active sites to be closer, and creates steric hindrance, which deters the catalyst activity. The results of XRD can support this attribution as NS posing the better dispersion of vanadium modifiers on its surface than MS.

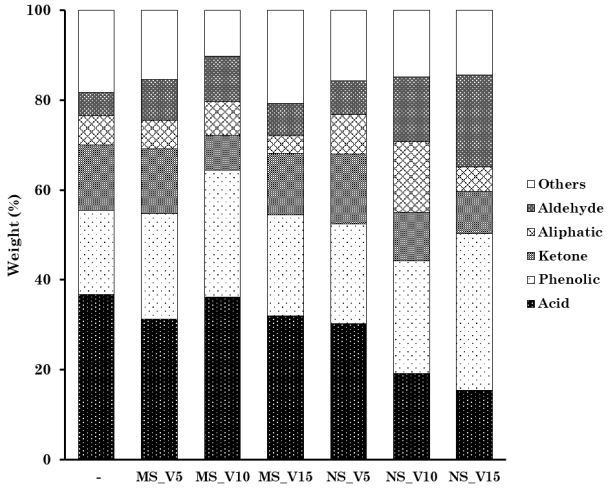

Figure 5. Selected compounds in the bio-oils obtained from various catalysts.

The effect of different surface area of the silica support on the catalytic performance has previously found in the copolymerization of ethylene and 1-hexene (comonomer) [45]. It showed that silica with the larger surface area produced copolymers with the higher comonomer incorporation, suggesting to more space between the active sites on its surface for the large molecules of comonomer attacking.

The almost constant solid yields were resulted from the solid product forming in the reactor without direct contact with the catalyst [35], and thus no catalytic reactions involve with the solid formation. Nevertheless, the solid formation may be taken place under high pressure of vapor which generated above reaction zone but only inside the reactor as the same for all run, not relating to the catalyst.

The bulk acidity of the catalyst measured with the titration method were nearly the same, and not directly related to the catalytic activity. Surface acidity should be further determined for better explanation of the result. Nevertheless, from the literature [25], it was found that the higher content of vanadium could lead to the higher acidy as observed in vanadium contained H-MCM-41 catalysts, and then the higher acidity enhanced deoxygenation (decarbonylation and decarboxylation) during the biomass catalytic pyrolysis. This is in consistent with this study as seen that the catalytic reaction was intensified with the higher content of vanadium.

3.3 Bio-oil Characterization

The compositional analysis of the obtained bio-oils was performed using GC-MS measurement. The detected compounds were classified into 4 main groups (acid, phenolic, ketone, aliphatic and aldehyde) and 1 other group including furan, sugar, amide, alcohol *etc.*, as shown in Figure 5.

It was obviously seen that the amounts of acid compounds were relatively low in the bio-oils obtained with the NS catalyst, and decreased with increasing the vanadium content in the catalyst. The decrease of acid content in the bio-oils agrees with the decrease of bio-oil yields. This is probably because the acid compounds were removed as gas via the catalytic reaction generated with the nanocatalysts, for example, the decomposition of acetic acid to methane and carbon dioxide (reaction 4). The amounts of acetic acid in the bio-oils as shown in Table 2 also supports this assumption.

$$CH_3COOH \rightarrow CH_4 + CO_2 \quad (4)$$

In addition, transformation of acetic acid in the bio-oil into other useful product e.g. H_2 has been proposed by many literatures, using catalytic steam reforming (CSR) through the reaction as follows:

$$CH_3COOH + 2H_2O \rightarrow 4H_2 + 2CO_2 \quad (5)$$

The catalysts used for CSR included Al_2O_3 supported with Pt, Pd, Rh, Ru, and Ni [46]; Co/SBA-15 supported with Cu, Ag, Ce, and Cr [47]; and also rice husk silica supported with Ni [34], or as a source for hydroxy-sodalite zeolite [48]. This indicated that rice husk silica has the potential to perform CSR during the pyrolysis and could reduce the amount of acetic acid as observed in this study. The suitable condition for CSR may be spontaneously created inside the pyrolysis system here with the high moisture content in the pomelo peels.

Phenolic compounds contents in the bio-oils were all higher with the catalysts, especially NS_V15. In general, the decomposition of lignin of the feed stock generates phenolic compounds, mostly alkylated phenols. Further reactions through the catalysts such as decarboxylation, oligomerization, decarboxylation, demethoxylation, and demethylation could turn the alkylated phenols into phenols [49]. From Table 2, it can be seen that both the amounts of phenolic compounds and the phenol increased with the catalysts. This suggests that the reactions, which promote the decomposition of lignin component and conversion to phenol, were both enhanced with the catalysts. The ability to convert phenolic compounds to phenol for all systems was also shown in Table 2, and was found that it dramatically increased with the nanosilica catalyst.

Other nano-oxide *i.e.* NiO, ZnO and Cu_2O have also previously shown the high ability in phenol production from the biomass pyrolysis [50]. The characteristic of nanoparticles may be suitable for the catalytic reaction favoring the phenol production. The opposite was true in our previous study with the synthesized ZSM-5 catalyst [14], which found that the phenol content in the obtained bio-oil decreased with the catalyst. Besides the difference in the catalyst types, the *in situ* catalytic method of that work (mixing catalyst and biomass together in the reactor) also differs from this study. For *in situ* system, the catalyst is immersed to a concentrated stream of pyrolysis vapors, thus having more opportunity to oligomerize to larger aromatic compounds at acid sites, thus decreasing the phenol composition in the bio-oil. Therefore, the method of catalytic pyrolysis was also the crucial factor to determine the chemical compositions of the obtained bio-oil.

Table 2. Chemical composition, conversion of phenol and heating value of the bio-oils from various catalyst.

Run	Catalyst	Compound			Conversion to phenol (%)	Heating value (MJ/kg)
		Acetic acid	Phenolic compounds	Phenol		
1	-	33.1	18.7	5.3	28.4	25.83
2	MS_V5	28.5	23.6	6.1	25.9	26.45
3	MS_V10	32.9	28.2	11.1	39.3	28.07
4	MS_V15	29.6	22.4	7.2	32.1	27.23
5	NS_V5	30.3	22.2	10.0	45.0	26.68
6	NS_V10	12.2	25.0	11.1	44.4	26.96
7	NS_V15	7.9	34.8	18.1	52.0	26.61

For the aldehyde contents in bio-oil, they varied considerably among all catalysts. In fact, it has been found previously that the vanadium in silica supports exhibited some selectivity toward aldehyde formation through the Mars van Krevelen (MvK) mechanism [24]. This was due to a moderate to high M−O bond strength in the vanadium oxide, creating oxygen vacancies by partial reduction, and then favoring MvK mechanism. Therefore, in this study the other effects could be more profound than the effect of M−O bond strength of the vanadium which benefits aldehyde production.

The heating value of the bio-oils from the catalytic pyrolysis slightly increased compared with the conventional pyrolysis, as shown in Table 2. The highest heat value (28.07 MJ/kg) belonged to the bio-oils with MS_V10, resulted from the high number of aliphatic compounds, and low contents of ketones and aldehydes. An increase of heating values with the catalyst has also been found in our previous study [51] with ZSM-5 synthesized from rice husk, which increased the heating value from 22.26 to 24.78 MJ/kg. This can confirm that the rice husk has the potential in using as a precursor for preparing the catalyst, which is efficiently used in the catalytic pyrolysis system. Nevertheless, as mentioned above the purity of the silica from the rice hulk (natural resources) should be aware, and also the process to produce the subsequent nanomaterial.

When comparing the heating values of the bio-oil of a variety of biomass from non-catalytic pyrolysis (Table 3), it was found that the bio-oils derived from the pomelo peels in this study is comparable to the others. Therefore, the pyrolysis of pomelo peels is an interesting way in utilization of the agricultural residue, and conversion into valuable bio-oil products. For the bio-oil yields, it was seen that they greatly vary between the variation of biomass. This is resulted from the composition of the biomass, which is an important factor in determining the bio-oil yield, especially the ratio of cellulose and hemicellulose [52].

4. Conclusion

Rice husk was used for preparation of MS and NS modified with vanadium (5-15 wt%) for used as catalysts in the pyrolysis of pomelo peels. It was found that non-catalytic pyrolysis pomelo peels provided the bio-oil yield of 33.3 wt%. When introducing the catalysts into the pyrolysis systems, it decreased the bio-yields due to the occurrence of the second reactions, which leads to the conversion of bio-oil into gas product. For NS catalyst, increasing the amount of vanadium loading directly decrease the bio-oil yields and increase the gas yield. In addition, NS exhibited higher efficiency in reducing the acid content in the bio-oil, and increasing the phenol content than MS. The distinguished properties of the nanoparticles may be the main reason for these phenomena.

Acknowledgment

This research is funded by National Research Council of Thailand. The authors thank Center of Excellence in Glass Technology and Materials Science (CEGM), Nakhon Pathom Rajabhut University for the XRF measurement, and Center of Excellence on Catalysis and Catalytic Reaction Engineering: Chulalongkorn University for the XRD and BET measurement.

Table 3. Bio-oil yields and heating values of the bio-oils obtained from the pyrolysis of various biomass.

Biomass	Temperature (°C)	Bio-oil yield (wt%)	Heating value (MJ/kg)	Ref.
Pomelo peels	500	33.3	25.83	This study
Eucalyptus wood	480	30.0	21.4	[53]
Cassava rhizome	472	63.23	26.9	[54]
Sugarcane bagasse	499	64.6	29.15	[55]
Sugarcane leaves	403	53.4	27.44	[55]
Sugarcane tops	402	52.2	25.48	[55]
Forest residue	450	53.3	22-27	[56]
Jackfruit peel	550	52.6	29.3	[57]
Napier grass	480	32.97	19.79	[58]
Cassia pods	400	33.16	21.36	[10]

CRediT Author Statement

Author Contribution: **K. Boongcharoenlab**: Investigation, Resources; **I. Tongdang**: Investigation, Resources; **W. Kiatkittipong**: Review and Editing; **A. Jaturapiree**: Conceptualization, Methodology, Investigation, Resources, Data Curation, Writing, Review and Editing, Supervision; **K. Sukrat**: Conceptualization, Methodology; **T. Saowapark**: Conceptualization, Methodology; **E. Chaichana**: Conceptualization, Validation, Review and Editing. All authors have read and agreed to the published version of the manuscript.

References

[1] Varma, V.S., Yadav, J., Das, S., Kalamdhad, A.S. (2015). Potential of waste carbide sludge addition on earthworm growth and organic matter degradation during vermicomposting of agricultural wastes. *Ecological Engineering*, 83, 90-95. DOI: 10.1016/j.ecoleng.2015.05.050.

[2] Karak, T., Sonar, I., Nath, J.R., Paul, R.K., Das, S., Boruah, R.K., Dutta, A.K., Das, K. (2015). Struvite for composting of agricultural wastes with termite mound: Utilizing the unutilized. *Bioresource Technology*, 187, 49-59. DOI: 10.1016/j.biortech.2015.03.070.

[3] Wang, B., Dong, F., Chen, M., Zhu, J., Tan, J., Fu, X., Wang, Y., Chen, S. (2016). Advances in Recycling and Utilization of Agricultural Wastes in China: Based on Environmental Risk, Crucial Pathways, Influencing Factors, Policy Mechanism. *Procedia Environmental Sciences*, 31, 12-17. DOI: 10.1016/j.proenv.2016.02.002.

[4] Trisdge, (5 March 2023). Production of Fresh Pomelo. https://www.tridge.com/intelligences/pomelo/production.

[5] Zain, N.F.M., Yusop, S.M., Ahmad, I. (2015) Preparation and Characterization of Cellulose and Nanocellulose From Pomelo (Citrus grandis) Albedo. *Journal of Nutrition & Food Sciences*, 5, 334. DOI: 10.4172/2155-9600.1000334

[6] Zain, N., Mohamad Yusop, S., Ahmad, I. (2013). *Cellulose Nanocrystal from Pomelo (C-Grandis Osbeck) Albedo: Chemical, Morphology and Crystallinity Evaluation*. Vol. 1571, 674-679.

[7] He, C., Li, H., Hong, J., Xiong, H., Ni, H., Zheng, M. (2022). Characterization and Functionality of Cellulose from Pomelo Fruitlets by Different Extraction Methods. *Polymers,* 14(3), 518. DOI: 10.3390/polym14030518.

[8] Siamphan, C., Arnthong, J., Tharad, S., Zhang, F., Yang, J., Laothanachareon, T., Chuetor, S., Champreda, V., Zhao, X.-Q., Suwannarangsee, S. (2022). Production of D-galacturonic acid from pomelo peel using the crude enzyme from recombinant Trichoderma reesei expressing a heterologous exopolygalacturonase gene. *Journal of Cleaner Production*, 331, 129958. DOI: 10.1016/j.jclepro.2021.129958.

[9] Gani, A., Naruse, I. (2007). Effect of cellulose and lignin content on pyrolysis and combustion characteristics for several types of biomass. *Renewable Energy*, 32(4), 649-661. DOI: 10.1016/j.renene.2006.02.017.

[10] Wongsawiang, O., Unpipat, M., Chareannate, C., Chaichana, E. (2016). Pyrolysis of agricultural residues in the local area of Nakhon Pathom Province. *Interdisciplinary Research Review*, 11(3), 46-53. DOI: 10.14456/jtir.2016.1.

[11] Durange, J.A., Santos, M.R., Pereira, M.M., Fernandes Jr, L.A., Souza, M.N., Mendes, A.N., Mesa, L.M., Sánchez, C.G., Sanchez, E.M., Pérez, J.M. (2013). Physicochemical properties of pyrolysis bio-oil from sugarcane straw and sugarcane in Natura. *Journal of Biomaterials and Nanobiotechnology*, 4(02), 10. DOI: 10.4236/jbnb.2013.42A002.

[12] French, R., Czernik, S. (2010). Catalytic pyrolysis of biomass for biofuels production. *Fuel Processing Technology*, 91(1), 25-32. DOI: 10.1016/j.fuproc.2009.08.011.

[13] Bardalai, M., Mahanta, D.K. (2016). Characterisation of the pyrolysis oil derived from bael shell (aegle marmelos). *Environmental Engineering Research*, 21(2), 180-187. DOI: 10.4491/eer.2015.142.

[14] Boongcharoenlab, K., Tongdang, J., Jaturapiree, A., Sukrat, K., Saowapark, T., Chaichana, E. (2021). Catalytic pyrolysis of various agricultural residues over ZSM-5 derived from rice husk silica. *Research Journal of Chemistry and Environment*, 25(6), 118-128.

[15] López, A., de Marco, I., Caballero, B.M., Laresgoiti, M.F., Adrados, A., Torres, A. (2011). Pyrolysis of municipal plastic wastes II: Influence of raw material composition under catalytic conditions. *Waste Management*. 31(9), 1973-1983. DOI: 10.1016/j.wasman.2011.05.021.

[16] Lee, K.-H. (2009). Thermal and catalytic degradation of pyrolytic oil from pyrolysis of municipal plastic wastes. *Journal of Analytical and Applied Pyrolysis*, 85(1), 372-379, DOI: 10.1016/j.jaap.2008.11.032.

[17] Hernández, M.D.R., Gómez, A., García, Á.N., Agulló, J., Marcilla, A. (2007). Effect of the temperature in the nature and extension of the primary and secondary reactions in the thermal and HZSM-5 catalytic pyrolysis of HDPE. *Applied Catalysis A: General*, 317(2), 183-194. DOI: 10.1016/j.apcata.2006.10.017.

[18] Lee, K.-H. (2012). Effects of the types of zeolites on catalytic upgrading of pyrolysis wax oil. *Journal of Analytical and Applied Pyrolysis*, 94(Supplement C), 209-214. DOI: 10.1016/j.jaap.2011.12.015.

[19] Sarker, M., Kabir, A., Rashid, M.M., Molla, M., Mohammad, A.S.M.D. (2011). Waste polyethylene terephthalate (PETE-1) conversion into liquid fuel. *Journal of Fundamentals of Renewable Energy and Applications*. 1(2011), R101202. DOI: 10.4303/jfrea/R101202.

[20] Li, P., Niu, B., Pan, H., Zhang, Y., Long, D. (2023). Production of hydrocarbon-rich bio-oil from catalytic pyrolysis of waste cooking oil over nickel monoxide loaded corn cob-derived activated carbon. *Journal of Cleaner Production*, 384, 135653. DOI: 10.1016/j.jclepro.2022.135653.

[21] Zeng, Z., Tian, X., Wang, Y., Cui, X., Zhang, Q., Dai, L., Liu, Y., Zou, R., Chen, J., Liu, J., Ruan, R. (2021). Microwave-assisted catalytic pyrolysis of corn cobs with Fe-modified Choerospondias axillaris seed-based biochar catalyst for phenol-rich bio-oil. *Journal of Analytical and Applied Pyrolysis*, 159, 105306. DOI: 10.1016/j.jaap.2021.105306.

[22] Wang, L., Si, B., Han, X., Yi, W., Li, Z., Zhang, A. (2022). Study on the effect of red mud and its component oxides on the composition of bio-oil derived from corn stover catalytic pyrolysis. *Industrial Crops and Products*, 184, 114973. DOI: 10.1016/j.indcrop.2022.114973.

[23] Saowapark, T., Sombatsompop, N., Sirisinha, C. (2009). Viscoelastic properties of fly ash-filled natural rubber compounds: Effect of fly ash loading. *Journal of Applied Polymer Science*, 112(4), 2552-2558. DOI: 10.1002/app.29700.

[24] Kantarelis, E., Yang, W., Blasiak, W. (2014). Effects of Silica-Supported Nickel and Vanadium on Liquid Products of Catalytic Steam Pyrolysis of Biomass. *Energy & Fuels*, 28(1), 591-599. DOI: 10.1021/ef401939g.

[25] Kim, B.-S., Jeong, C.S., Kim, J.M., Park, S.B., Park, S.H., Jeon, J.-K., Jung, S.-C., Kim, S.C., Park, Y.-K. (2016). Ex situ catalytic upgrading of lignocellulosic biomass components over vanadium contained H-MCM-41 catalysts. *Catalysis Today*, 265, 184-191. DOI: 10.1016/j.cattod.2015.08.031.

[26] Bo-ongcharoenlab, K., Rungngam, J., Khadthiphong, A., Pimpakhun, K., Kaewbuadee, J., Chaichana, E. (2018). Catalytic pyrolysis of water hyacinth with rice husk-derived silica modified by vanadium. *Journal of Materials Science and Applied Energy*, 7(3), 345 - 351.

[27] Chaichana, E., Jongsomjit, B., Praserthdam, P. (2007). Effect of nano-SiO2 particle size on the formation of LLDPE/SiO2 nanocomposite synthesized via the in situ polymerization with metallocene catalyst. *Chemical Engineering Science*, 62(3), 899-905. DOI: 10.1016/j.ces.2006.10.005.

[28] Arianpour, F., Jahangiri, M., Abedi, S., Vafaee, F., Yousif, Q.A., Salavati-Niasari, M. (2022). In-situ polymerization of silica/polyethylene using bisupported Ziegler-Natta catalyst of nanosilica/BOM/TiCl4/TEAL: Study of thermo-mechanical properties system. *Inorganic Chemistry Communications*, 143, 109726. DOI: 10.1016/j.inoche.2022.109726.

[29] Chong, C.C., Cheng, Y.W., Bahari, M.B., Teh, L.P., Abidin, S.Z., Setiabudi, H.D. (2021). Development of nanosilica-based catalyst for syngas production via CO2 reforming of CH4: A review. *International Journal of Hydrogen Energy*, 46(48), 24687-24708. DOI: 10.1016/j.ijhydene.2020.01.086.

[30] Mirante, F., Gomes, N., Branco, L.C., Cunha-Silva, L., Almeida, P.L., Pillinger, M., Gago, S., Granadeiro, C.M., Balula, S.S. (2019). Mesoporous nanosilica-supported polyoxomolybdate as catalysts for sustainable desulfurization. *Microporous and Mesoporous Materials*, 275, 163-171. DOI: 10.1016/j.micromeso.2018.07.036.

[31] Gogoi, N., Gogoi, P.K., Borah, G., Bora, U. (2016). Grafting of Ru(III) complex onto nanosilica and its implication as heterogeneous catalyst for aerobic oxidative hydroxylation of arylboronic acids. *Tetrahedron Letters*, 57(36), 4050-4052. DOI: 10.1016/j.tetlet.2016.07.070.

[32] Salakhum, S., Yutthalekha, T., Chareonpanich, M., Limtrakul, J., Wattanakit, C. (2018). Synthesis of hierarchical faujasite nanosheets from corn cob ash-derived nanosilica as efficient catalysts for hydrogenation of lignin-derived alkylphenols. *Microporous and Mesoporous Materials*, 258, 141-150. DOI: 10.1016/j.micromeso.2017.09.009.

[33] Aldosari, O.F. (2019). Selective conversion of furfuryl alcohol to 2-methylfuran over nanosilica supported Au:Pd bimetallic catalysts at room temperature. *Journal of Saudi Chemical Society*, 23(7), 938-946. DOI: 10.1016/j.jscs.2019.04.004.

[34] Guo, W., Li, G., Zheng, Y., Li, K. (2021). Nano-silica extracted from rice husk and its application in acetic acid steam reforming. *RSC Advances*, 11(55), 34915-34922. DOI: 10.1039/D1RA05255A.

[35] Tan, Y.L., Abdullah, A.Z., Hameed, B.H. (2018). Catalytic fast pyrolysis of durian rind using silica-alumina catalyst: Effects of pyrolysis parameters. *Bioresource Technology*, 264, 198-205. DOI: 10.1016/j.biortech.2018.05.058.

[36] Rahman, I.A.,Padavettan, V. (2012). Synthesis of Silica Nanoparticles by Sol-Gel: Size-Dependent Properties, Surface Modification, and Applications in Silica-Polymer Nanocomposites—A Review. *Journal of Nanomaterials*, 2012, 132424. DOI: 10.1155/2012/132424.

[37] Rabiei, M., Palevicius, A., Dashti, A., Nasiri, S., Monshi, A., Vilkauskas, A., Janusas, G. (2020). Measurement modulus of elasticity related to the atomic density of planes in unit cell of crystal lattices. *Materials*, 13(19), 4380. DOI: 10.3390/ma13194380.

[38] Occhiuzzi, M., Cordischi, D., Dragone, R. (2005). Reactivity of some vanadium oxides: An EPR and XRD study. *Journal of Solid State Chemistry*, 178(5), 1551-1558. DOI: 10.1016/j.jssc.2005.02.019.

[39] Fang, S., Yu, Z., Ma, X., Lin, Y., Chen, L., Liao, Y. (2018). Analysis of catalytic pyrolysis of municipal solid waste and paper sludge using TG-FTIR, Py-GC/MS and DAEM (distributed activation energy model). *Energy*, 143, 517-532. DOI: 10.1016/j.energy.2017.11.038.

[40] Al Mohamadi, H., Aljabri, A., Mahmoud, E.R.I., Khan, S.Z., Aljohani, M.S., Shamsuddin, R. (2021). Catalytic pyrolysis of municipal solid waste: effects of pyrolysis parameters. *Bulletin of Chemical Reaction Engineering & Catalysis*, 16(2), 342-352. DOI: 10.9767/bcrec.16.2.10499.342-352.

[41] Maneechakr, P.,Karnjanakom, S. (2021). Improving the bio-oil quality via effective pyrolysis/deoxygenation of palm kernel cake over a metal (Cu, Ni, or Fe)-doped carbon catalyst. *ACS Omega*, 6(30), 20006-20014. DOI: 10.1021/acsomega.1c02999.

[42] Gupta, S., Lanjewar, R., Mondal, P. (2022). Enhancement of hydrocarbons and phenols in catalytic pyrolysis bio-oil by employing aluminum hydroxide nanoparticle based spent adsorbent derived catalysts. *Chemosphere*, 287, 132220. DOI: 10.1016/j.chemosphere.2021.132220.

[43] Ghaemy, M., Bazzar, M., Mighani, H. (2011). Effect of nanosilica on the kinetics of cure reaction and thermal degradation of epoxy resin. *Chinese Journal of Polymer Science*, 29, 141-148. DOI: 10.1007/s10118-010-1003-9.

[44] Gun'ko, V., Voronin, E., Nosach, L., Turov, V., Wang, Z., Vasilenko, A., Leboda, R., Skubiszewska-Zięba, J., Janusz, W., Mikhalovsky, S. (2011). Structural, textural and adsorption characteristics of nanosilica mechanochemically activated in different media. *Journal of Colloid and Interface Science*, 355(2), 300-311. DOI: 10.1016/j.jcis.2010.12.008.

[45] Chaichana, E., Khaubunsongserm, S., Praserthdam, P., Jongsomjit, B. (2011). Effect of Ga modification on different pore size silicas in synthesis of LLDPE by copolymerization of ethylene and 1-hexene with [t-BuNSiMe2Flu]TiMe2/MMAO catalyst. *Polymer Bulletin,* 66(9), 1301-1312. DOI: 10.1007/s00289-010-0433-4.

[46] Basagiannis, A.C., Verykios, X.E. (2007). Catalytic steam reforming of acetic acid for hydrogen production. *International Journal of Hydrogen Energy*, 32(15), 3343-3355. DOI: 10.1016/j.ijhydene.2007.04.039.

[47] Megía, P.J., Carrero, A., Calles, J.A., Vizcaíno, A.J. (2019). Hydrogen Production from Steam Reforming of Acetic Acid as a Model Compound of the Aqueous Fraction of Microalgae HTL Using Co-M/SBA-15 (M: Cu, Ag, Ce, Cr) Catalysts. *Catalysts*, 9(12), 1013. DOI: 10.3390/catal9121013.

[48] Pandiangan, K.D., Simanjuntak, W., Avista, D., Arinanda, A.G., Hadi, S., Amrulloh, H. (2022). Synthesis of Hydroxy-Sodalite from Rice Husk Silica and Food-Grade Aluminum Foil as A Catalyst for Biomass Pyrolysis. *Trends in Sciences*, 19(20), 6252. DOI: 10.48048/tis.2022.6252.

[49] Kim, J.-Y., Lee, J.H., Park, J., Kim, J.K., An, D., Song, I.K., Choi, J.W. (2015). Catalytic pyrolysis of lignin over HZSM-5 catalysts: Effect of various parameters on the production of aromatic hydrocarbon. *Journal of Analytical and Applied Pyrolysis*, 114, 273-280. DOI: 10.1016/j.jaap.2015.06.007.

[50] Rajić, N., Logar, N.Z., Rečnik, A., El-Roz, M., Thibault-Starzyk, F., Sprenger, P., Hannevold, L., Andersen, A., Stöcker, M. (2013). Hardwood lignin pyrolysis in the presence of nano-oxide particles embedded onto natural clinoptilolite. *Microporous and Mesoporous Materials*, 176, 162-167. DOI: 10.1016/j.micromeso.2013.04.005.

[51] Neumlang, P., Khadthiphong, A., Pimpakhun, K., Kaewbuadee, J., Chaichana, E. (2018). Low acid bio-oil from para rubber seeds produced via catalytic pyrolysis with V-modified silica catalyst. *Food and Applied Bioscience Journal*, 6, 135-147.

[52] Zhang, L., Dou, X., Yang, Z., Yang, X., Guo, X. (2021). Advance in hydrothermal bio-oil preparation from lignocellulose: effect of raw materials and their tissue structures. *Biomass*, 1(2), 74-93. DOI: 10.3390/biomass1020006.

[53] Mendoza-Martinez, C., Sermyagina, E., Saari, J., Ramos, V.F., Vakkilainen, E., Cardoso, M., Alves Rocha, E.P. (2023). Fast oxidative pyrolysis of eucalyptus wood residues to replace fossil oil in pulp industry. *Energy*, 263, 126076. DOI: 10.1016/j.energy.2022.126076.

[54] Suttibak, S., Sriprateep, K., Pattiya, A. (2012). Production of bio-oil via fast pyrolysis of cassava rhizome in a fluidised-bed reactor. *Energy Procedia*, 14, 668–673. DOI: 10.1016/j.egypro.2011.12.993.

[55] Suttibak, S. (2017). Influence of reaction temperature on yields of bio-oil from fast pyrolysis of sugarcane residues. *Engineering and Applied Science Research*, 44(3), 142-147.

[56] Vamvuka, D., Esser, K., Marinakis, D. (2023). Characterization of pyrolysis products of forest residues and refuse-derived fuel and evaluation of their suitability as bioenergy sources. *Applied Sciences*, 13(3), 1482. DOI: 10.3390/app13031482.

[57] Soetardji, J.P., Widjaja, C., Djojorahardjo, Y., Soetaredjo, F.E., Ismadji, S. (2014). Bio-oil from Jackfruit Peel Waste. *Procedia Chemistry*, 9, 158-164. DOI: 10.1016/j.proche.2014.05.019.

[58] Suntivarakorn, R., Treedet, W., Singbua, P., Teeramaetawat, N. (2018). Fast pyrolysis from Napier grass for pyrolysis oil production by using circulating Fluidized Bed Reactor: Improvement of pyrolysis system and production cost. *Energy Reports*, 4, 565-575. DOI: 10.1016/j.egyr.2018.08.004.